NIH Public Access
Author Manuscript
Biochemistry. Author manuscript; available in PMC 2012 March 29.

Published in final edited form as:
Biochemistry. 2011 March 29; 50(12): 2235–2242. doi:10.1021/bi1018607.

Robust self-association is a common feature of mammalian visual arrestin-1

Miyeon Kim[1,#], **Susan M. Hanson**[2,3,#], **Sergey A. Vishnivetskiy**[2,#], **Xiufeng Song**[2], **Whitney M. Cleghorn**[2], **Wayne L. Hubbell**[1,*], and **Vsevolod V. Gurevich**[2,*]

[1] University of California Los Angeles, Los Angeles, CA 90095

[2] Vanderbilt University, Nashville, TN 37232

Abstract

Arrestin-1 binds light-activated phosphorhodopsin and ensures rapid signal termination. Its deficiency in humans and mice results in prolonged signaling and rod degeneration. However, most of the biochemical studies were performed on bovine arrestin-1, which was shown to self-associate forming dimers and tetramers, although only the monomer binds rhodopsin. It is unclear whether self-association is a property of arrestin-1 in all mammals, or a specific feature of bovine protein. To address this issue, we compared self-association parameters of purified human and mouse arrestin-1 with those of bovine counterpart using multi-angle light scattering. We found that mouse and human arrestin-1 also robustly self-associate, existing in monomer-dimer-tetramer equilibrium. Interestingly, the combination of dimerization and tetramerization constants in these three species is strikingly different. While tetramerization of bovine arrestin-1 is highly cooperative, with $K_{D,dim}{}^4 > K_{D,tet}$, in mouse $K_{D,dim} \sim K_{D,tet}$, whereas in human $K_{D,dim} \ll K_{D,tet}$. Importantly, in all three species at very high physiological concentrations of arrestin-1 in rod photoreceptors, most of it is predicted to exist in oligomeric form, with relatively low concentration of free monomer. Thus, it appears that maintenance of low levels of active monomer is the biological role of arrestin-1 self-association.

Keywords

arrestin-1; self-association; mutagenesis; photoreceptor; vision

Arrestin-1[4] binds light-activated rhodopsin phosphorylated by GRK1 (a.k.a. rhodopsin kinase) with high affinity (1), ensuring the termination of light-induced signaling with sub-second kinetics (2). Arrestin-1 knockout in mice dramatically slows the photoresponse shutoff in rod (3) and cone (4) photoreceptors. Arrestin-1 deficiency in humans results in Oguchi disease, a form of stationary night blindness (5). Arrestin-1 is expressed at very high levels in both photoreceptor types, being the second most abundant signaling protein after corresponding opsins (4,6,7). Considering that the rhodopsin concentration in rod outer segments (OS) is ~3 mM (8), the average cytoplasmic concentration of arrestin-1 (which is

[*]Corresponding authors: Vsevolod V. Gurevich, Department of Pharmacology, Vanderbilt University, Nashville, TN 37232; Tel: 615-322-7070; FAX: 615-343-6532; vsevolod.gurevich@vanderbilt.edu, Wayne L. Hubbell, Jules Stein Eye Institute and Department of Chemistry and Biochemistry, University of California Los Angeles, Los Angeles, CA 90095; Tel: 310-206-8830; FAX: 310-794-2144; hubbellw@jsei.ucla.edu.

[3]Present address: Carroll University, Waukesha, WI 53186

[#]These authors equally contributed to this work

[4]We use systematic names of arrestin proteins: arrestin-1 (a.k.a. visual or rod arrestin, 48 kDa protein, or S-antigen), arrestin-2 (β-arrestin or β-arrestin1), arrestin-3 (β-arrestin2), and arrestin-4 (cone or X-arrestin).

NIH-PA Author Manuscript
NIH-PA Author Manuscript
NIH-PA Author Manuscript

NIH-PA Author Manuscript

NIH-PA Author Manuscript

NIH-PA Author Manuscript

expressed at ~0.8:1 ratio to rhodopsin (6,7,9)) is expected to be >1 mM (1). Dark-adapted rods are used in most studies of the molecular mechanisms of rod signaling in genetically modified mice (reviewed in (10–12)). In the dark, ~85% of arrestin-1 resides in the inner segments, cell bodies, and synaptic terminals (6,9,13–15), which brings its concentration in these compartments to >2 mM (9). While the majority of the functional studies were performed in mice and humans, the biochemical properties of arrestin-1 were mostly studied using bovine protein. Bovine arrestin-1 robustly self-associates (16,17), cooperatively forming dimers and tetramers (16,18,19). It is unclear whether this is a peculiar property of bovine protein, or a common feature of mammalian arrestin-1 species. In addition, since only monomeric arrestin-1 binds rhodopsin and quenches the signaling (18), the concentration of the monomer is an important functional parameter; it can be calculated based on total arrestin-1 if the self-association constant(s) are known. In view of therapeutic potential of “enhanced” mutants that can compensate for deficits of rhodopsin phosphorylation *in vivo* (20), characterization of human arrestin-1 is particularly important. Therefore, we explored oligomerization of purified mouse and human arrestin-1 and found that self-association is a common feature of mammalian arrestin-1. Interestingly, we found that while the values of dimerization and tetramerization constants of arrestin-1 from three species are very different, the underlying molecular interactions appear to be similar: the same point mutations render bovine and mouse arrestin-1 constitutively monomeric.

Methods

Materials

[γ-^{32}P]ATP, [^{14}C]leucine, and [^{3}H]leucine were purchased from DuPont NEN. All restriction enzymes were purchased from New England Biolabs. Sepharose 2B and all other chemicals were from sources previously described (21,22). Rabbit reticulocyte lysate was purchased from Ambion, and SP6 RNA polymerase was prepared as previously described (23). 11-*cis*-retinal was generously supplied by Dr. R. K. Crouch and the National Eye Institute.

Site-directed mutagenesis

Bovine, mouse, and human arrestin-1 cDNA were cloned into pGEM2-based plasmid with an "idealized" 5'-untranslated region (23) under control of a SP6 promoter. All mutations were introduced by PCR using an appropriate mutagenizing oligonucleotide as a forward primer and an oligonucleotide downstream from the far restriction site to be used for subcloning as a reverse primer. Resulting fragments of various lengths and an appropriate primer upstream of the near restriction site were then used as reverse and forward primers, respectively, for the second round of PCR. Resulting fragments were subcloned back, and all constructs were confirmed by dideoxynucleotide sequencing.

In vitro transcription, translation, and evaluation of mutants’ stability

Plasmids were linearized with Hind III before *in vitro* transcription to produce mRNAs encoding full-length arrestin proteins, as described (22,24). All arrestin proteins were labeled by incorporation of [^{3}H]leucine and [^{14}C]leucine with the specific activity of the mix being 1.5–3 Ci/mmol, resulting in the specific activity of arrestin proteins within the range of 66-85 Ci/mmol (145-187 dpm/fmol). The translation of every protein produced a single labeled band with the expected mobility on SDS-PAGE. The relative stability of all mutants used in this study (evaluated as described in (25)) exceeds 90% of corresponding wild type arrestin.

NIH-PA Author Manuscript

NIH-PA Author Manuscript

NIH-PA Author Manuscript

Rhodopsin preparations

Urea-treated rod OS membranes were prepared, phosphorylated with rhodopsin kinase and regenerated with 11-*cis*-retinal as described (21). The stoichiometry of phosphorylation for the rhodopsin preparations used in these studies was 3.7 mol phosphate/mol rhodopsin.

Direct binding assays

Arrestin-1 binding to rhodopsin was performed, as described (24,26). Briefly, *in vitro* translated tritiated arrestins (100 fmol) were incubated in 50 mM Tris-HCl, pH 7.5, 0.5 mM $MgCl_2$, 1.5 mM dithiothreitol, 50 mM potassium acetate with 7.5 pmol (0.3 μg) of the various functional forms of rhodopsin in a final volume of 50 μl for 5 min at 37°C either in the dark or under room light. The samples were immediately cooled on ice and loaded under dim red light onto 2 ml Sepharose 2B columns equilibrated with 10 mM Tris-HCl, pH 7.5, 100 mM NaCl. Bound arrestin eluted with the disc membranes in the void volume (between 0.5 – 1.1 ml). Nonspecific binding determined in the presence of 0.3 μg liposomes was subtracted. Arrestin-1 binding to microtubules (MT) (purified tubulin polymerized in the presence of taxol) was performed, as described (27). Briefly, 200 femtomoles of the indicated *in vitro* translated arrestins were incubated in 50 mM Tris-HCl, pH 7.4, 0.5 mM $MgCl_2$, 1.5 mM DTT, 1 mM EGTA, and 50 mM potassium acetate for 20 min at 25°C with 20 μg of pre-polymerized tubulin. MTs along with bound arrestin were pelleted. MT-arrestin pellets were not washed due to the low affinity (i.e. high off-rate) of the interaction. The pellet was dissolved in 0.1 ml of 1% SDS, 50 mM NaOH, and bound arrestin was quantified by liquid scintillation counting. Non-specific "binding" (arrestin pelleted without microtubules) was subtracted.

Arrestin-1 purification and analysis of its self-association

WT and mutant mouse, WT bovine, and WT human arrestin-1 were expressed in *E. coli* and purified, essentially as described (22). All light scattering measurements were made with a DAWN EOS detector coupled to an Optilab refractometer (Wyatt Technologies) following gel filtration on a 7.8 mm (ID) × 30.0 cm (L) silica-based column along with its guard column (Wyatt Technologies). The arrestin samples (100 μl) at different concentrations were incubated in fresh 5 mM DTT for 30 min at room temperature to disrupt covalent inter-arrestin disulfide bonds and injected onto the column at 25°C, at a flow rate of 0.8 ml/min in 50 mM MOPS, 100 mM NaCl, pH 7.2. The column used did not resolve oligomeric species, but simply acted as a filter to remove highly scattering particulates. Light scattering at 18 angles (15°–160°), absorbance at 280 nm, and refractive index (at 690 nm) for each sample were taken for a slice centered at the peak of the elution profile and of width approximately that of the profile at half maximum (18). The experimental weight-averaged molecular weight values were obtained from the protein concentration and light scattering data using ASTRA 5.3.4.16 software (Wyatt Technologies). The weight-averaged molecular weight data were analyzed using the two-step monomer-dimer-tetramer (MDT) model (16),

$$2M \overset{K_{dim}}{\longleftrightarrow} D \quad 2D \overset{K_{tet}}{\longleftrightarrow} T$$

where M, D, and T are monomer, dimer, and tetramer, respectively. Details of the analysis have been previously described (28). Except where noted, the equilibrium constants are given in terms of the corresponding dissociation constants, $K_{D,dimer}$ ($K_{D,dim}$) and $K_{D,\ tetramer}$ ($K_{D,tet}$). The errors in equilibrium constants were determined from least-squares fitting of the data to MDT model, taking into account an estimated error of ± 1 kDa is the computed values of the average molecular weight (28).

NIH-PA Author Manuscript

NIH-PA Author Manuscript

NIH-PA Author Manuscript

Results

The level of arrestin-1 in photoreceptors (4,6,7,9) is three orders of magnitude higher than the level of non-visual arrestins in other neurons (29,30). Another characteristic feature of arrestin-1 is robust self-association at physiological concentrations (16–18). Since all previous studies of arrestin-1 self-association were performed with bovine protein, we tested whether WT mouse arrestin-1 uses the same oligomerization mechanism. To this end, we expressed mouse arrestin-1 in *E. coli*, purified it, and tested its self-association by measuring the dependence of the average molecular weight on its concentration by multi-angle light scattering. We found that mouse arrestin-1 forms dimers and tetramers (Fig. 1A) like its bovine homolog (18). Although both dimerization ($K_{D,dim}$=57.5±0.6 μM) and especially tetramerization ($K_{D,tet}$=63.1±2.6 μM) constants are higher than corresponding values for bovine arrestin-1 (37.2±0.2 μM and 7.4±0.1 μM, respectively (18)), at physiological concentrations of >2 mM (1,9) only a small fraction of WT mouse arrestin-1 would be monomeric (Fig. 1B). Interestingly, while tetramerization of bovine arrestin-1 was invariably found to be cooperative (16,18,19), i.e., $K_{D,dim} > K_{D,tet}$, the mouse protein has virtually equal $K_{D,dim}$ and $K_{D,tet}$, indicating a lack of cooperativity in self-association (Table 1).

The significant difference between self-association constants of bovine and mouse arrestin-1 prompted us to analyze the human homologue (Fig. 1C,D). We found that purified human arrestin-1 also self-associates, with remarkably low $K_{D,dim}$=2.95±0.02 μM and relatively high $K_{D,tet}$=224±5 μM (Table 1). Interestingly, these disparate sets of constants in the three mammalian species yield predicted levels of the monomer in the cell body of dark-adapted rod at ~2 mM total arrestin-1 concentration (extrapolating measured mouse values (8, 9) to other species) in the relatively narrow range of 30–90 μM (Table 2). Total tetramer concentrations vary by only 30% (Table 2). The main difference is in the resulting dimer levels, which varies almost 5-fold, from predicted 59 μM in bovine to 281 μM in human rod (Table 2).

The value of measured $K_{D,dim}$ between human and mouse arrestin-1 shows ~20-fold difference, and the value of $K_{D,tet}$ between bovine and human proteins differs by ~30-fold. These dramatic differences raise the possibility that the three mammalian arrestin-1 species could use distinct interaction interfaces, so that common self-association phenotype could represent convergent evolution, rather than direct conservation. It has been recently shown that the structure of the solution tetramer of bovine arrestin-1 is different from that of the crystal tetramer (18). Extensive investigation yielded a model of the solution tetramer, where receptor-binding surfaces are shielded by “sister” subunits, which explains demonstarted inability of the oligomers to bind rhodopsin (19). Based on this model, a modified bovine arrestin-1 was constructed, where two (F85A,F197A) mutations predicted to disrupt NN (F85A) and CC (F197A) self-association interfaces were introduced (Fig. 2A,B,C) (19). Indeed, this mutant was shown to be essentially monomeric, with $K_{D,dim}$=525 μM and no detectable tetramer formation (19), independently confirming the model. To test whether the same subunit arrangement is present in the tetramer of mouse arrestin-1, we introduced homologous mutations (F86A,F198A), expressed this protein, and measured its self-association. We found that this mutation in mouse arrestin-1 yields the same non-self-associating phenotype as in its bovine counterpart, demonstrating $K_{D,dim}$=537 μM and no detectable tetramerization (Fig. 2D). Further disruption of the CC interface by the addition of an A349V mutation brought $K_{D,dim}$ to 724 μM (Fig. 2D; Table 1). Thus, homologous mutations in bovine and mouse arrestin-1 affect their self-association in a similar manner, suggesting that the same interfaces are involved in oligomerization of both proteins, and the difference in constants reflects the relative energy of interactions between the subunits, rather than a global difference in the structure of the solution tetramer.

NIH-PA Author Manuscript

NIH-PA Author Manuscript

NIH-PA Author Manuscript

Phosphorylated light-activated rhodopsin (P-Rh*) is the main binding target of arrestin-1 in the rod (31). The amount of rhodopsin present in the OS determines the amount of arrestin-1 that can translocated to this compartment (7), supporting the idea that rhodopsin binding holds arrestin-1 in the OS in the light (14). In contrast, in the dark most of arrestin-1 (the estimates for WT mouse range from ~85% (9) to 91% (6) - >95% (7,14)) resides in other compartments of the cell (6,13–15), where it is anchored *via* low-affinity binding to microtubules (14,32,33) abundant in the inner segment, perinuclear area, and synaptic terminals (34). Therefore, to test whether observed differences in self-association are the result of selective disruption of the interfaces involved, we compared the binding of WT and mutant forms of bovine and mouse arrestin-1 to P-Rh* and *in vitro* polymerized microtubules (Fig. 3). Using fully functional radiolabeled arrestins and standard direct binding assays (22,27,32,35) we found that mutations that disrupt oligomerization in bovine and mouse arrestin-1 do not appreciably affect the binding to either partner (Fig. 3A,B). Arrestin-1 is a highly sensitive molecule, where even small conformational perturbations by mutagenesis result in dramatic changes of its binding to P-Rh* (20,25,26,36–40) and microtubules (27,32). Thus, virtually wild type binding to both rhodopsin and microtubules makes it highly unlikely that these mutations induce any global structural changes in the molecule, leaving targeted disruption of the self-association interfaces as the only plausible explanation of their phenotype.

Discussion

Preferential binding of arrestin-1 to P-Rh* (41) and resulting quenching of rhodopsin signaling (42) were discovered in mid-1980s, and this remains its least controversial function to this day (1). The ability of bovine arrestin-1 (under the name of S-antigen) to self-associate was discovered a decade earlier (43), but no biological function was ascribed to this phenomenon. The interest in arrestin-1 self-association was revived when two crystal structures of bovine protein (44,45) revealed virtually identical tetramers. Further studies confirmed its self-association in solution (16–18), although careful examination revealed that the structure of the solution tetramer that forms under much more physiological conditions is dramatically different from that found in crystal (18,19). The oligomers were usually discussed as storage forms, an interpretation strongly supported by direct demonstration that only the monomer is capable of binding P-Rh* (18). Yet it remained unclear why out of all signaling proteins present at enormous (as compared to other neurons) concentrations in the rod (8), arrestin-1 is the only one that has a special apparently inactive storage form. Since all these studies were performed on bovine protein, it was not even clear whether self-association is a common feature of mammalian arrestin-1 species, which would be the case if it has physiologically relevant function.

Here we compared arrestin-1 from three mammals: (1) bovine, traditionally used for biochemical studies; (2) mouse, the best functionally characterized *in vivo*; and (3) human, the most therapeutically relevant. In each case we found that arrestin-1 robustly self-associates at physiological concentrations, which suggests that this feature is biologically important. Surprisingly, the thermodynamics of self-association in the three species are strikingly different. While tetramerization of bovine arrestin-1 is cooperative, in a sense that $K_{D,dim} > K_{D,tet}$, there is no such cooperativity in mouse ($K_{D,dim} \sim K_{D,tet}$), whereas in human $K_{D,dim} \ll K_{D,tet}$, being 10- and 20-times lower than $K_{D,dim}$ of bovine and mouse arrestin-1, respectively (Table 1). Despite these differences, the structures of the solution tetramers are likely similar, as judged by remarkably uniform effects of mutations destabilizing inter-subunit interfaces in bovine and mouse arrestin-1 (Fig. 2; Table 1). Importantly, these mutations do not appreciably affect arrestin-1 binding to P-Rh* and microtubules (Fig. 3), suggesting that the conservation of the interface residues reflects the need for self-association, rather than being a byproduct of conservation of other arrestin-1 functions. Most

NIH-PA Author Manuscript

NIH-PA Author Manuscript

NIH-PA Author Manuscript

of the residues in the self-association interfaces identified in bovine arrestin-1 (19) and deduced by homology modeling in mouse and human proteins are conserved, with a few differences possibly responsible for distinct thermodynamics.

Rod photoreceptors function in dim light, saturating even at modest illumination levels (46). Thus, clues to possible biological functions of arrestin-1 self-association may be revealed through its effects on the state of arrestin-1 at concentrations found in the dark-adapted rod. Arrestin-1 distribution in dark-adapted rods was quantitatively measured only in mouse (6,7,9,14). However, rod function in different mammals is similar, and arrestin-1/rhodopsin ratios in the OS of dark-adapted mouse (9) and frog (47) rods are remarkably close. Therefore, mouse expression levels were used for all species in the estimates that follow. In the dark the bulk (85–95% (6,7,9,14)) of arrestin-1 is localized to the cell body, where expected concentration reaches ~2 mM, with much lower concentration of ~300 μM in the OS, where its main target rhodopsin is localized (9). Using these concentrations and measured values of K_D (Table 1), we estimated the expected equilibrium concentrations of arrestin-1 monomer, dimer, and tetramer in the dark-adapted rod (Table 2). In all three cases, arrestin-1 self-association makes the fraction of the monomer in the cell body relatively small, 1.5–4.7%. However, each species achieves this result in a somewhat different way (Tables 1, 2). In case of bovine protein, self-association is cooperative, with $K_{D,tet} < K_{D,dim}$, so that at 2 mM the bulk (>90%) of arrestin-1 is stored in the form of tetramer, while the fraction of the dimer is very small (<6%). In mouse, $K_{D,dim} \sim K_{D,tet}$, so that while the bulk (~80%) is still a tetramer, much larger fraction (~16%) exists as a dimer. Human arrestin-1 dimerizes more readily than the others, but shows less robust tetramerization, so that at the same concentration only 70% exists as a tetramer, whereas as much as 28% is a dimer. In all cases monomer concentration is <100 μM, with about 3-fold differences among species, dimer concentrations vary ~5-fold, whereas absolute tetramer levels vary by only ~30% (Table 2).

Light exposure induces massive arrestin-1 translocation from the inner segment and cell body to the OS, which takes up to 30–60 min (6,13–15,48,49). Considering that the photoresponse, which is normally terminated with sub-second kinetics (2,50–52), is greatly prolonged in arrestin-1 knockout animals (3), arrestin-1 present in the OS in the dark must be responsible for timely shutoff. Our analysis of arrestin-1 oligomerization suggests that level of the monomer, which is the only rhodopsin-binding form (18), is much higher in the OS (>50 μM) in nocturnal mice most reliant on rod vision, compared to <30 μM in bovine and just ~16 μM in human rods. Rod vision is less crucial for these latter diurnal species.

Using the second-order on-rate constant (k_1) recently measured for arrestin-1 binding to P-Rh* (~10^6 $M^{-1}s^{-1}$ for P-Rh* in nanodiscs (53)) along with the monomer concentration allows one to estimate the expected pseudo-first order rate constant for an encounter of rhodopsin with arrestin-1 (k_1x[monomeric arrestin-1]), which in mouse yields ~50 s^{-1}. This estimate of the lower limit suggests that each rhodopsin encounters an arrestin-1 molecule on average once every ~20 ms. In other words, arrestin-1 “checks” the functional state of rhodopsin in this time interval and binds tightly when it encounters P-Rh* (1). Again, this yields an estimate of a lower limit to the active rhodopsin lifetime in mouse rods, which must be >20 ms because of additional time that GRK1 needs to attach three or more phosphates to light-activated rhodopsin necessary for the high-affinity arrestin-1 binding (21,52). This number is consistent with the original experimental estimate of <60 ms (2) and more recent one of ~30 ms (51), as well as with the modeling of photoresponse dynamics based on these data (54,55). By the same token, lower monomer concentrations in the OS of bovine and human rods (Table 2) suggest that the lifetime of the active rhodopsin in these species must be longer, >36 ms and >65 ms, respectively. Since in the OS arrestin-1 diffuses in the cytoplasm with complex geometry (56), while rhodopsin diffuses in two dimensions

NIH-PA Author Manuscript

NIH-PA Author Manuscript

NIH-PA Author Manuscript

on the disc membrane, the actual on-rate could differ from these estimates, so these predictions need to be tested experimentally.

Several studies showed that light-dependent translocation of arrestin-1 to the OS (14), as well as transducin movement out of the OS (57), is energy-independent, largely driven by their interactions with non-moving partners (reviewed in (58)), whereas others suggested that active transport could be involved (59,60). Arrestin-1 in photoreceptors is clearly at disequilibrium in the dark and in bright light (61). Thus, regardless of the mode of transportation, it must be "tethered" in the OS in the light and in the cell body in the dark by other proteins. Otherwise, the diffusion would quickly undo anything that active transport could achieve. Therefore, the concentrations of free monomer, dimer, and tetramer in the OS and cell body are likely equal (1). Preferential arrestin-1 localization outside of the OS in the dark was reported to be determined by its binding to microtubules (14,33), abundant in the cell body and sparse in the OS (34). Other arrestin-1 binding partners, such as N-ethylmaleimide-sensitive factor (NSF, (62)) and/or enolase (63) could also serve as anchors in the cell body in the dark. However, the concentration of polymerized tubulin, where each αβ-dimer can bind arrestin-1 (27), by far exceeds all other putative anchors combined, suggesting that MTs likely serve as the main binding partner. Thus, the difference in the concentration of each form between these two compartments of the rod largely reflects its MT-associated fraction. The size of the rods and their OS are significantly different in different species. Unfortunately, the volume of the cytoplasm in the OS and other rod compartments, as well as the concentrations of rhodopsin and other signaling molecules, was carefully measured only in mice and frogs (64). However, arrestin-1/rhodopsin ratios in dark-adapted mouse OS (9) and ~20 times larger frog OS (47) are remarkably close. On the strength of these findings and the fact that the size of the OS is determined by the amount of rhodopsin present there (65), the estimates below are based on the assumption that arrestin-1 concentration in dark-adapted mammalian rods is similar. In this case, in all species the predicted levels of the monomer, dimer, and tetramer in the cell body exceed those in the OS by 1.7–1.9-fold, ~3-fold, and ~10-fold, respectively (Table 2). In bright light, much higher total arrestin-1 concentration in the OS was shown to be due to its binding to rhodopsin (6,7,14), as the amount of rhodopsin in the OS clearly limits molar amount of arrestin-1 that can translocate to this compartment (7). Similarly, in the dark the total concentration of each form of arrestin-1 in the cell body likely exceeds corresponding value in the OS by the amount that is bound to MTs. For example, in mouse rod the estimated total concentration of monomer is 52.8 μM in the OS and 95 μM in the cell body (Table 2). The latter exceeds the OS concentration by ~42 μM, suggesting that this amount (~44% of the total monomeric arrestin-1 in this compartment) is bound to MTs. Similarly calculated differences in the concentrations of monomer, dimer, and tetramer in the OS and the cell body suggest that the fractions of the individual MT-bound forms in the cell body are fairly close in the three mammalian species: monomer (40–47%), dimer (65–71%), and tetramer (87–91%). However, each of the three molecular forms of arrestin-1 apparently has distinct propensity to associate with MTs, with the order of potency being: tetramer ≫ dimer ≫ monomer.

To conclude, here we show that arrestin-1 self-association is conserved in three mammalian species, indicating that this phenomenon is biologically important. We present evidence that, although the dimerization and tetramerization equilibrium constants are very different in the three species examined, the overall structures of the solution tetramers are likely to be very similar. Despite the differences in thermodynamics of association, for each species the concentration of the active monomer is very low, while the bulk of arrestin-1 exists in the form of tetramer with the best ability to bind microtubules in the cell body. The concentrations of the arrestin-1 monomer in the OS, estimated from the oligomerization equilibrium constants, provide experimentally testable predictions regarding the lifetime of active rhodopsin in different species. An "enhanced" arrestin-1 mutant with increased

NIH-PA Author Manuscript

NIH-PA Author Manuscript

NIH-PA Author Manuscript

affinity for light-activated unphosphorylated rhodopsin was recently shown to have therapeutic potential in genetic disorders with deficient rhodopsin phosphorylation (20). The biological importance of arrestin-1 self-association indicates that the changes in self-association, inadvertently produced by mutagenesis, may underlie reported deleterious effects of very high expression of this mutant (20). Thus, normal ability of any mutant form of arrestin-1 to oligomerize must be ascertained before it can be used for gene therapy.

Acknowledgments

We are grateful to Drs. T. Shinohara, C. M. Craft, and W. C. Smith for bovine, mouse, and human arrestin-1 cDNA, respectively, to Dr. R. K. Crouch and the National Eye Institute for 11-cis-retinal, and to Dr. Christian Altenbach for the Labview programs used in the analysis of the light scattering data and for assistance in their use.

Funding: NIH grants EY011500, GM077561, GM081756 (VVG), EY05216 and the Jules Stein Professorship Endowment (WLH), and training grant EY007135 (WMC).

Abbreviations

K_{dim} (=1/$K_{D,dim}$)	dimerization constant, i.e., equilibrium association constant of two arrestin-1 monomers
K_{tet} (=1/$K_{D,tet}$)	tetramerization constant, i.e., equilibrium association constant of two arrestin-1 dimers
GRK1	G protein-coupled receptor kinase 1, a.k.a. rhodopsin kinase
P-Rh*	phosphorylated light-activated rhodopsin

References

1. Gurevich, VV.; Hanson, SM.; Gurevich, EV.; Vishnivetskiy, SA. How rod arrestin achieved perfection: regulation of its availability and binding selectivity. In: Kisselev, O.; Fliesler, SJ., editors. Methods in Signal Transduction Series. CRC Press; Boca Raton: 2007. p. 55-88.
2. Krispel CM, Chen D, Melling N, Chen YJ, Martemyanov KA, Quillinan N, Arshavsky VY, Wensel TG, Chen CK, Burns ME. RGS expression rate-limits recovery of rod photoresponses. Neuron. 2006; 51:409–416. [PubMed: 16908407]
3. Xu J, Dodd RL, Makino CL, Simon MI, Baylor DA, Chen J. Prolonged photoresponses in transgenic mouse rods lacking arrestin. Nature. 1997; 389:505–509. [PubMed: 9333241]
4. Nikonov SS, Brown BM, Davis JA, Zuniga FI, Bragin A, Pugh EN Jr, Craft CM. Mouse cones require an arrestin for normal inactivation of phototransduction. Neuron. 2008; 59:462–474. [PubMed: 18701071]
5. Fuchs S, Nakazawa M, Maw M, Tamai M, Oguchi Y, Gal A. A homozygous 1-base pair deletion in the arrestin gene is a frequent cause of Oguchi disease in Japanese. Nat Genet. 1995; 10:360–362. [PubMed: 7670478]
6. Strissel KJ, Sokolov M, Trieu LH, Arshavsky VY. Arrestin translocation is induced at a critical threshold of visual signaling and is superstoichiometric to bleached rhodopsin. J Neurosci. 2006; 26:1146–1153. [PubMed: 16436601]
7. Hanson SM, Gurevich EV, Vishnivetskiy SA, Ahmed MR, Song X, Gurevich VV. Each rhodopsin molecule binds its own arrestin. Proc Nat Acad Sci USA. 2007; 104:3125–3128. [PubMed: 17360618]
8. Pugh, EN., Jr; Lamb, TD. Phototransduction in vertebrate rods and cones: Molecular mechanisms of amplification, recovery and light adaptation. In: Stavenga, DG.; DeGrip, WJ.; Pugh, EN., Jr, editors. Handbook of Biological Physics. Molecular Mechanisms in Visual Transduction. Elsevier; Amsterdam: 2000. p. 183-255.

NIH-PA Author Manuscript

NIH-PA Author Manuscript

NIH-PA Author Manuscript

9. Song X, Vishnivetskiy SA, Seo J, Chen J, Gurevich EV, Gurevich VV. Arrestin-1 expression level in rods: balancing functional performance and photoreceptor health. Neuroscience. 2011; 174:37–49. [PubMed: 21075174]
10. Burns ME, Arshavsky VY. Beyond counting photons: trials and trends in vertebrate visual transduction. Neuron. 2005; 48:387–401. [PubMed: 16269358]
11. Bok D. Contributions of genetics to our understanding of inherited monogenic retinal diseases and age-related macular degeneration. Arch Ophthalmol. 2007; 125:160–164. [PubMed: 17296891]
12. Makino CL, Wen XH, Lem J. Piecing together the timetable for visual transduction with transgenic animals. Curr Opin Neurobiol. 2003; 13:404–412. [PubMed: 12965286]
13. Broekhuyse RM, Tolhuizen EF, Janssen AP, Winkens HJ. Light induced shift and binding of S-antigen in retinal rods. Curr Eye Res. 1985; 4:613–618. [PubMed: 2410196]
14. Nair KS, Hanson SM, Mendez A, Gurevich EV, Kennedy MJ, Shestopalov VI, Vishnivetskiy SA, Chen J, Hurley JB, Gurevich VV, Slepak VZ. Light-dependent redistribution of arrestin in vertebrate rods is an energy-independent process governed by protein-protein interactions. Neuron. 2005; 46:555–567. [PubMed: 15944125]
15. Elias RV, Sezate SS, Cao W, McGinnis JF. Temporal kinetics of the light/dark translocation and compartmentation of arrestin and alpha-transducin in mouse photoreceptor cells. Mol Vis. 2004; 10:672–681. [PubMed: 15467522]
16. Imamoto Y, Tamura C, Kamikubo H, Kataoka M. Concentration-dependent tetramerization of bovine visual arrestin. Biophys J. 2003; 85:1186–1195. [PubMed: 12885662]
17. Schubert C, Hirsch JA, Gurevich VV, Engelman DM, Sigler PB, Fleming KG. Visual arrestin activity may be regulated by self-association. J Biol Chem. 1999; 274:21186–21190. [PubMed: 10409673]
18. Hanson SM, Van Eps N, Francis DJ, Altenbach C, Vishnivetskiy SA, Klug CS, Hubbell WL, Gurevich VV. Structure and function of the visual arrestin oligomer. EMBO J. 2007; 26:1726–1736. [PubMed: 17332750]
19. Hanson SM, Dawson ES, Francis DJ, Van Eps N, Klug CS, Hubbell WL, Meiler J, Gurevich VV. A model for the solution structure of the rod arrestin tetramer. Structure. 2008; 16:924–934. [PubMed: 18547524]
20. Song X, Vishnivetskiy SA, Gross OP, Emelianoff K, Mendez A, Chen J, Gurevich EV, Burns ME, Gurevich VV. Enhanced Arrestin Facilitates Recovery and Protects Rod Photoreceptors Deficient in Rhodopsin Phosphorylation. Curr Biol. 2009; 19:700–705. [PubMed: 19361994]
21. Vishnivetskiy SA, Raman D, Wei J, Kennedy MJ, Hurley JB, Gurevich VV. Regulation of arrestin binding by rhodopsin phosphorylation level. J Biol Chem. 2007; 282:32075–32083. [PubMed: 17848565]
22. Gurevich VV, Benovic JL. Arrestin: mutagenesis, expression, purification, and functional characterization. Methods Enzymol. 2000; 315:422–437. [PubMed: 10736718]
23. Gurevich VV. Use of bacteriophage RNA polymerase in RNA synthesis. Methods Enzymol. 1996; 275:382–397. [PubMed: 9026651]
24. Gurevich VV, Benovic JL. Cell-free expression of visual arrestin. Truncation mutagenesis identifies multiple domains involved in rhodopsin interaction. J Biol Chem. 1992; 267:21919–21923. [PubMed: 1400502]
25. Gurevich VV. The selectivity of visual arrestin for light-activated phosphorhodopsin is controlled by multiple nonredundant mechanisms. J Biol Chem. 1998; 273:15501–15506. [PubMed: 9624137]
26. Hanson SM, Gurevich VV. The differential engagement of arrestin surface charges by the various functional forms of the receptor. J Biol Chem. 2006; 281:3458–3462. [PubMed: 16339758]
27. Hanson SM, Cleghorn WM, Francis DJ, Vishnivetskiy SA, Raman D, Song S, Nair KS, Slepak VZ, Klug CS, Gurevich VV. Arrestin mobilizes signaling proteins to the cytoskeleton and redirects their activity. J Mol Biol. 2007; 368:375–387. [PubMed: 17359998]
28. Hanson SM, Vishnivetskiy SA, Hubbell WL, Gurevich VV. Opposing effects of inositol hexakisphosphate on rod arrestin and arrestin2 self-association. Biochemistry. 2008; 47:1070–1075. [PubMed: 18161994]

NIH-PA Author Manuscript

NIH-PA Author Manuscript

NIH-PA Author Manuscript

29. Gurevich EV, Benovic JL, Gurevich VV. Arrestin2 and arrestin3 are differentially expressed in the rat brain during postnatal development. Neuroscience. 2002; 109:421–436. [PubMed: 11823056]
30. Gurevich EV, Benovic JL, Gurevich VV. Arrestin2 expression selectively increases during neural differentiation. J Neurochem. 2004; 91:1404–1416. [PubMed: 15584917]
31. Gurevich VV, Gurevich EV. The molecular acrobatics of arrestin activation. Trends Pharmacol Sci. 2004; 25:105–111. [PubMed: 15102497]
32. Hanson SM, Francis DJ, Vishnivetskiy SA, Klug CS, Gurevich VV. Visual arrestin binding to microtubules involves a distinct conformational change. J Biol Chem. 2006; 281:9765–9772. [PubMed: 16461350]
33. Nair KS, Hanson SM, Kennedy MJ, Hurley JB, Gurevich VV, Slepak VZ. Direct binding of visual arrestin to microtubules determines the differential subcellular localization of its splice variants in rod photoreceptors. J Biol Chem. 2004; 279:41240–41248. [PubMed: 15272005]
34. Eckmiller MS. Microtubules in a rod-specific cytoskeleton associated with outer segment incisures. Vis Neurosci. 2000; 17:711–722. [PubMed: 11153651]
35. Gurevich VV, Benovic JL. Visual arrestin interaction with rhodopsin: Sequential multisite binding ensures strict selectivity towards light-activated phosphorylated rhodopsin. J Biol Chem. 1993; 268:11628–11638. [PubMed: 8505295]
36. Gurevich VV, Benovic JL. Visual arrestin binding to rhodopsin: diverse functional roles of positively charged residues within the phosphorylation-recignition region of arrestin. J Biol Chem. 1995; 270:6010–6016. [PubMed: 7890732]
37. Gurevich VV, Benovic JL. Mechanism of phosphorylation-recognition by visual arrestin and the transition of arrestin into a high affinity binding state. Mol Pharmacol. 1997; 51:161–169. [PubMed: 9016359]
38. Gray-Keller MP, Detwiler PB, Benovic JL, Gurevich VV. Arrestin with a single amino acid sustitution quenches light-activated rhodopsin in a phosphorylation-independent fasion. Biochemistry. 1997; 36:7058–7063. [PubMed: 9188704]
39. Vishnivetskiy SA, Paz CL, Schubert C, Hirsch JA, Sigler PB, Gurevich VV. How does arrestin respond to the phosphorylated state of rhodopsin? J Biol Chem. 1999; 274:11451–11454. [PubMed: 10206946]
40. Vishnivetskiy SA, Schubert C, Climaco GC, Gurevich YV, Velez M-G, Gurevich VV. An additional phosphate-binding element in arrestin molecule: implications for the mechanism of arrestin activation. J Biol Chem. 2000; 275:41049–41057. [PubMed: 11024026]
41. Kuhn H, Hall SW, Wilden U. Light-induced binding of 48-kDa protein to photoreceptor membranes is highly enhanced by phosphorylation of rhodopsin. FEBS Lett. 1984; 176:473–478. [PubMed: 6436059]
42. Wilden U, Hall SW, Kühn H. Phosphodiesterase activation by photoexcited rhodopsin is quenched when rhodopsin is phosphorylated and binds the intrinsic 48-kDa protein of rod outer segments. Proc Natl Acad Sci USA. 1986; 83:1174–1178. [PubMed: 3006038]
43. Wacker WB, Donoso LA, Kalsow CM, Yankeelov JAJ, Organisciak DT. Experimental allergic uveitis. Isolation, characterization, and localization of a soluble uveitopathogenic antigen from bovine retina. J Immunol. 1977; 119:1949–1958. [PubMed: 334977]
44. Granzin J, Wilden U, Choe HW, Labahn J, Krafft B, Buldt G. X-ray crystal structure of arrestin from bovine rod outer segments. Nature. 1998; 391:918–921. [PubMed: 9495348]
45. Hirsch JA, Schubert C, Gurevich VV, Sigler PB. The 2. A crystal structure of visual arrestin: a model for arrestin's regulation. Cell. 1999; 97:257–269. [PubMed: 10219246]
46. Pugh, EN., Jr; Falsini, B.; Lyubarsky, AL. The origin of the major rod- and cone-driven components of the rodent electroretinogram, and the effect of age and light-rearing history on the magnitudes of these components. In: Williams, TP.; Thistle, AB., editors. Photostasis and Related Phenomena. Plenum Press; New York: 1998. p. 93-128.
47. Hamm HE, Bownds MD. Protein complement of rod outer segments of frog retina. Biochemistry. 1986; 25:4512–4523. [PubMed: 3021191]
48. Philp NJ, Chang W, Long K. Light-stimulated protein movement in rod photoreceptor cells of the rat retina. FEBS Lett. 1987; 225:127–132. [PubMed: 2826235]

NIH-PA Author Manuscript

NIH-PA Author Manuscript

NIH-PA Author Manuscript

49. Whelan JP, McGinnis JF. Light-dependent subcellular movement of photoreceptor proteins. J Neurosci Res. 1988; 20:263–270. [PubMed: 3172281]
50. Burns ME, Mendez A, Chen CK, Almuete A, Quillinan N, Simon MI, Baylor DA, Chen J. Deactivation of phosphorylated and nonphosphorylated rhodopsin by arrestin splice variants. J Neurosci. 2006; 26:1036–1044. [PubMed: 16421323]
51. Gross OP, Burns ME. Control of rhodopsin's active lifetime by arrestin-1 expression in mammalian rods. J Neurosci. 2010; 30:3450–3457. [PubMed: 20203204]
52. Mendez A, Burns ME, Roca A, Lem J, Wu LW, Simon MI, Baylor DA, Chen J. Rapid and reproducible deactivation of rhodopsin requires multiple phosphorylation sites. Neuron. 2000; 28:153–164. [PubMed: 11086991]
53. Bayburt TH, Vishnivetskiy SA, McLean M, Morizumi T, Huang CC, Tesmer JJ, Ernst OP, Sligar SG, Gurevich VV. Rhodopsin monomer is sufficient for normal rhodopsin kinase (GRK1) phosphorylation and arrestin-1 binding. J Biol Chem. 2011; 286:1420–1428. [PubMed: 20966068]
54. Burns ME, Pugh ENJ. RGS9 concentration matters in rod phototransduction. Biophys J. 2009; 97:1538–1547. [PubMed: 19751658]
55. Caruso G, Bisegna P, Lenoci L, Andreucci D, Gurevich VV, Hamm HE, DiBenedetto E. Kinetics of rhodopsin deactivation and its role in recgulating recovery and reproducibility of rod photoresponse. PLoS Comput Biol. 2010; 6:e1001031. [PubMed: 21200415]
56. Bisegna P, Caruso G, Andreucci D, Shen L, Gurevich VV, Hamm HE, DiBenedetto E. Diffusion of the second messengers in the cytoplasm acts as a variability suppressor of the single photon response in vertebrate phototransduction. Biophys J. 2008; 94:3363–3383. [PubMed: 18400950]
57. Rosenzweig DH, Nair KS, Wei J, Wang Q, Garwin G, Saari JC, Chen CK, Smrcka AV, Swaroop A, Lem J, Hurley JB, Slepak VZ. Subunit dissociation and diffusion determine the subcellular localization of rod and cone transducins. J Neurosci. 2007; 27:5484–5494. [PubMed: 17507570]
58. Slepak VZ, Hurley JB. Mechanism of light-induced translocation of arrestin and transducin in photoreceptors: interaction-restricted diffusion. IUBMB Life. 2008; 60:2–9. [PubMed: 18379987]
59. Orisme W, Li J, Goldmann T, Bolch S, Wolfrum U, Smith WC. Light-dependent translocation of arrestin in rod photoreceptors is signaled through a phospholipase C cascade and requires ATP. Cell Signal. 2010; 22:447–456. [PubMed: 19887106]
60. Reidel B, Goldmann T, Giessl A, Wolfrum U. The translocation of signaling molecules in dark adapting mammalian rod photoreceptor cells is dependent on the cytoskeleton. Cell Motil Cytoskeleton. 2008; 65:785–800. [PubMed: 18623243]
61. Peet JA, Bragin A, Calvert PD, Nikonov SS, Mani S, Zhao X, Besharse JC, Pierce EA, Knox BE, Pugh EN Jr. Quantification of the cytoplasmic spaces of living cells with EGFP reveals arrestin-EGFP to be in disequilibrium in dark adapted rod photoreceptors. J Cell Sci. 2004; 117:3049–3059. [PubMed: 15197244]
62. Huang SP, Brown BM, Craft CM. Visual Arrestin acts as a modulator for N-ethylmaleimide-sensitive factor in the photoreceptor synapse. J Neurosci. 2010; 30:9381–9391. [PubMed: 20631167]
63. Smith WC, Bolch SN, Dugger DR, Li J, Esquenazi I, Arendt A, Benzenhafer D, McDowell JH. Interaction of arrestin with enolase1 in photoreceptors. Invest Ophthalmol Vis Sci. 2011 in press.
64. Shen L, Caruso G, Bisegna P, Andreucci D, Gurevich VV, Hamm HE, Dibenedetto E. Dynamics of mouse rod phototransduction and its sensitivity to variation of key parameters. IET Syst Biol. 2010; 4:12–32. [PubMed: 20001089]
65. Wen XH, Shen L, Brush RS, Michaud N, Al-Ubaidi MR, Gurevich VV, Hamm HE, Lem J, Dibenedetto E, Anderson RE, Makino CL. Overexpression of rhodopsin alters the structure and photoresponse of rod photoreceptors. Biophys J. 2009; 96:939–950. [PubMed: 19186132]

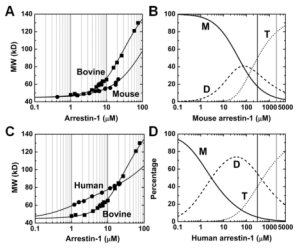

Fig. 1. Mouse and human arrestin-1 form dimers and tetramers at physiological concentrations

A. The average molecular weight of wild type mouse arrestin-1 as a function of total concentration (black circles) was determined from the light scattering data as described in the Methods. The solid curve is a least-squares fit of the data to the MDT model with $K_{D,dim}$ = 57.5±0.6 μM and $K_{D,tet}$ = 63.1±2.6 μM. The data for bovine arrestin-1 (18) are shown as squares for comparison. **B.** The percentage of mouse arrestin-1 molecules in monomer (M, straight line), dimer (D, dashed line), and tetramer (T, dotted line) as a function of total arrestin-1 concentration computed for the MDT model and the data in panel A. **C.** The average molecular weight of wild type human arrestin-1 as a function of total concentration (black circles) was determined from the light scattering data. The solid curve is a least-squares fit of the data to the MDT model with $K_{D,dim}$ = 2.95±0.02 μM and $K_{D,tet}$ =224±5 μM. **D.** The percentage of human arrestin-1 molecules in monomer (M, straight line), dimer (D, dashed line), and tetramer (T, dotted line) as a function of total arrestin-1 concentration computed for the MDT model and the data in panel **C.** Vertical lines in **B** and **D** correspond to arrestin-1 concentrations in the outer segment (300 μM, black) and cell body (2,000 μM, gray) of dark-adapted rod.

NIH-PA Author Manuscript NIH-PA Author Manuscript NIH-PA Author Manuscript

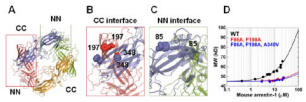

Fig. 2. The targeted disruption of arrestin-1 self-association

A. Solution tetramer structure of bovine arrestin-1 (19). Areas enlarged to show inter-subunit contacts are indicated. **B.** CC interface (between the two C-domains) showing the positions of residues F197 (F198 in mouse) and A348 (A349 in mouse). **C.** NN interface (between the two N-domains) showing the position of F85 (F86 in mouse). **D.** The average molecular weight of the F86A,F198A (red circles) and F86A,F198A,A349V (blue circles) mouse arrestin-1 mutants as a function of total arrestin concentration were determined from the light scattering data (symbols). The fit of the data to the MDT model (solid lines) was obtained, as described (18). Note that neither mutant showed detectable tetramerization, so that the resulting fit describes monomer-dimer equilibrium. The wild type (WT) mouse arrestin-1 data (black circles) are shown for comparison.

NIH-PA Author Manuscript
NIH-PA Author Manuscript
NIH-PA Author Manuscript

NIH-PA Author Manuscript

NIH-PA Author Manuscript

NIH-PA Author Manuscript

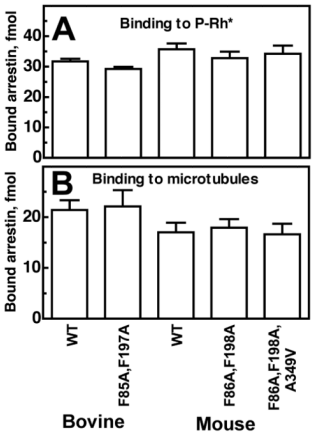

Fig. 3. Mutations disrupting self-association do not affect arrestin-1 binding to P-Rh* and microtubules

The binding of indicated radiolabeled arrestins to P-Rh* (100 fmol/assay) (**A**) and microtubules (200 fmol/assay) (**B**) was determined, as described in Methods. Means +/− SD of three experiments performed in duplicates are shown.

NIH-PA Author Manuscript

NIH-PA Author Manuscript

NIH-PA Author Manuscript

Table 1

Equilibrium constants characterizing self-association of WT and mutant mouse, human, and bovine arrestin-1.

Protein	log K_{dim} [a]	log K_{tet} [a]	$K_{D,dim}$, μM	$K_{D,tet}$, μM
Mouse arrestin-1	4.24±0.04	4.20±0.17	57.5±0.6	63.1±2.6
Mouse arrestin-1-(F86A,F198A)	3.27±0.05	-	537±9	-
Mouse arrestin-1-(F86A,F198A, A349V)	3.14±0.11	-	724±26	-
Human arrestin-1	5.53±0.03	3.65±0.08	2.95±0.02	224±5
Bovine arrestin-1	4.43±0.02	5.13±0.03	37.2±0.2	7.4±0.1
Bovine arrestin-1-(F85A,F197A)	3.28±0.10	-	525±16	-

[a] K_{dim} and K_{tet} are the *association* constants determined from light scattering analysis.

NIH-PA Author Manuscript

NIH-PA Author Manuscript

NIH-PA Author Manuscript

Table 2

Predicted concentrations of monomer, dimer, and tetramer of mouse, human, and bovine arrestin-1 at concentrations in the outer segment (300 μM) and cell body (2,000 μM) of dark-adapted rods.

Arrestin-1	Total, μM	Monomer, μM (%)	Dimer, μM (%)	Tetramer, μM (%)
Bovine	300	27.6 (9.2%)	20.8 (13.9%)	57.7 (76.9%)
Mouse	300	52.8 (17.6%)	48.8 (32.5%)	37.4 (49.9%)
Human	300	15.5 (5.2%)	82.1 (54.7%)	30.1 (40.1%)
Bovine	2,000	46 (2.3%)	59 (5.9%)	459 (91.8%)
Mouse	2,000	95 (4.7%)	159 (15.9%)	397 (79.4%)
Human	2,000	29 (1.5%)	281 (28.1%)	352 (70.4%)